INSTABILITY ZONES IDENTIFICATION IN MULTIBLADE ROTOR DYNAMICS

Leonardo Sanches, *leonardo.sanches@isae.fr*
Guilhem Michon, *guilhem.michon@isae.fr*
Université de Toulouse, ISAE – DMSM – CP: 31055, Toulouse, France

Alain Berlioz, *berlioz@cict.fr*
Université de Toulouse, INSA-UPS, LGMT, EA814 - 118 route de Narbonne, CP: 31 077, Toulouse, France

Daniel Alazard, *alazard@supaero.fr*
Université de Toulouse, ISAE – DMIA – CP: 31055, Toulouse, France

Abstract. *Helicopter ground resonance is an unstable dynamic phenomenon which can lead to the total destruction of the aircraft during take-off or landing phases. Studies have been developed by researchers which considered a simplified mathematical model. With the goal of further comprehend the phenomenon, predictions of unstable motions are done and compared. First, Floquet's theory is applied to solve the linear equations of motion including parametric and periodic terms. Then, the multiple scales method is applied on the nonlinear model. The analyses highlight that, by keeping the nonlinear terms in the equations, other instability zones are identified.*

Keywords: *Ground Resonance, Nonlinear Dynamics, Floquet Method, Multiple Scales Method.*

1. INTRODUCTION

The ground resonance phenomenon in helicopters consists of a self-excited oscillation caused by the interaction of the rotor blades' lagging motion with other helicopter modes of motion. Several accidents have been recorded and show that, under some conditions, it can be very violent and can lead to the total destruction of the aircraft.

Coleman and Feingold (1958) performed some of the earliest research on the phenomenon, and laid the foundation for all of the work that was to follow. Between those, Donham *et al.* (1969), and Lytwyn *et al.* (1969) studied this phenomenon taking into account also the air resonance effect. Major contributions in understanding the ground resonance phenomenon in hingeless and bearingless rotors were done by Army researchers, as for example, Dawson (1983) and Hodges (1979). Recently, Kunz (2002) analysed the influence of nonlinear springs and dampers (elastomeric elements) on predicting the rotor's instability zone. Byers and Gandhi (2006) explored the passive control of the problem.

However, in order to establish the criteria to avoid the unstable oscillations, the equations of motion were linearized and then simplified by eliminating the periodic and parametric termes. This last process, applicable only for isotropic systems, is identified as the Coleman Transformation and more generally called the multi blade coordinate transformation.

A recent study given by Skjoldan *et al.* (2009) kept the periodic and parametric terms in the equations of motion of a wind turbine. The instability zone predicted by using the Floquet's theory over a certain range of rotation speeds is similar to that predicted by Coleman and Feingold, for a isotropic rotor.

With the objective of further understanding the ground resonance phenomenon, an analysis of the nonlinear equations of motion is envisioned. This paper sets up the nonlinear equations of motion by considering all terms. Multiple scales method is used to treat the equations of motion.

2. MECHANICAL MODEL

Similar to that proposed by Coleman and Feingold, the present mechanical model is developed to characterize the dynamical behavior of a helicopter with a hinged rotor. In other words, it consists of figuring out the relation between the longitudinal – $x(t)$ - and lateral displacement – $y(t)$ - of the fuselage, and the k^{th} blade lag angle - $\varphi_k(t)$ – in terms of the rotor speed Ω and time t. Figure 1 illustrates a general schema of the system.

The fuselage is considered to be a rigid body with its center of gravity at point O. At the initial time, the origin of an inertial coordinate system (X_0,Y_0,Z_0) is coincident at this point. The body is connected to springs which represent the flexibility of the landing skid.

The rotor head system consists of an assembly of one rigid rotor hub with *Nb* blades. Each blade is represented by a concentrated mass located at a distance *b* from the lag articulation (point B) and, on each articulation, a torsional spring is present. The origin of a mobile coordinate system (x, y, z), parallel to the inertial one, is located at the geometric center of the rotor hub (point A). Both, body and rotor head, are joined by a rigid shaft and the aerodynamical forces on the blades are neglected.

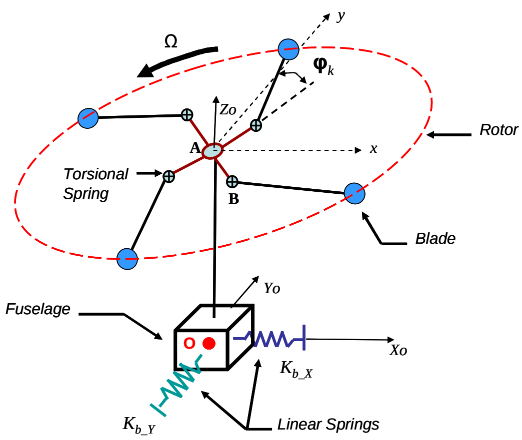

Figure 1. General schema of the mechanical model

2.1 Equation of motion

The equations of motion are obtained by applying Lagrange's equation on the kinetic and potential energy expressions of the system (body and rotor head). To reach this goal, some conditions have been considered, which are:

- The fuselage has mass m_f and the spring constants connected to it are $K_{f\text{-}X}$ and $K_{f\text{-}Y}$ through x and y directions, respectively;
- The rotor is composed of Nb = 4 blades and each blade k has an azimuth angle of $\theta_k = 2\pi(k-1)/Nb$ with the x - axis;
- Each blade has the same mass m_b and moment of inertia around the z - axis is to Iz_b;
- The angular spring constant for each k blade is $K_{b\text{-}k}$;
- The k blade position projected in the inertial coordinate system is:

$$x_{b\_k} = a\cos(\Omega t+\theta_k)+b\cos(\Omega t+\theta_k+\varphi_k(t))+x(t) \tag{1}$$

$$y_{b\_k} = a\sin(\Omega t+\theta_k)+b\sin(\Omega t+\theta_k+\varphi_k(t))+y(t) \tag{2}$$

where a is the hinge offset.

Considering the general Laplace variable **q** as

$$\{\mathbf{q}_{1..6}(t)\} = \{\, x(t)\quad y(t)\quad \varphi_1(t)\quad \varphi_2(t)\quad \varphi_3(t)\quad \varphi_4(t)\,\}^T = \{\mathbf{u}_{1..6}(t)\}^T \tag{3}$$

where **u** is a vector made up of the degree of freedom variables of the system.

Equations (4 - 6), are nonlinear equations in the function of **u**. Equations (4) and (5) correspond to the motion equation in the x and y directions, respectively. Equation (6) represents the dynamical equations of blades 1 to 4, changing n from 3 to 6 in that order.

$$\left(\frac{d^2}{dt^2}u_1(t)\right)+\omega_1^2\,u_1(t)$$
$$+\sum_{n=3}^{6}\left[\begin{array}{l} -r_m\,b\cos(\Omega t+\theta_{n-2})\sin(u_n(t))\left(\frac{d^2}{dt^2}u_n(t)\right)-r_m\,b\sin(\Omega t+\theta_{n-2})\cos(u_n(t))\left(\frac{d^2}{dt^2}u_n(t)\right) \\ -2\,\Omega\,r_m\,b\cos(\Omega t+\theta_{n-2})\cos(u_n(t))\left(\frac{d}{dt}u_n(t)\right)+2\,\Omega\,r_m\,b\sin(\Omega t+\theta_{n-2})\sin(u_n(t))\left(\frac{d}{dt}u_n(t)\right) \\ +r_m\,b\sin(\Omega t+\theta_{n-2})\sin(u_n(t))\left(\frac{d}{dt}u_n(t)\right)^2-r_m\,b\cos(\Omega t+\theta_{n-2})\cos(u_n(t))\left(\frac{d}{dt}u_n(t)\right)^2 \\ -\Omega^2\,r_m\,b\cos(\Omega t+\theta_{n-2})\cos(u_n(t))+\Omega^2\,r_m\,b\sin(\Omega t+\theta_{n-2})\sin(u_n(t)) \end{array}\right]=0 \tag{4}$$

$$\left(\frac{d^2}{dt^2}u_2(t)\right)+\omega_2^2\,u_2(t)$$
$$+\sum_{n=3}^{6}\begin{bmatrix} +r_m\,b\cos(\Omega t+\theta_{n-2})\cos(u_n(t))\left(\frac{d^2}{dt^2}u_n(t)\right)-r_m\,b\sin(\Omega t+\theta_{n-2})\sin(u_n(t))\left(\frac{d^2}{dt^2}u_n(t)\right) \\ -2\,\Omega\,\alpha\,b\cos(\Omega t+\theta_{n-2})\sin(u_n(t))\left(\frac{d}{dt}u_n(t)\right)-2\,\Omega\,r_m\,b\sin(\Omega t+\theta_{n-2})\cos(u_n(t))\left(\frac{d}{dt}u_n(t)\right) \\ -r_m\,b\sin(\Omega t+\theta_{n-2})\cos(u_n(t))\left(\frac{d}{dt}u_n(t)\right)^2-r_m\,b\cos(\Omega t+\theta_{n-2})\sin(u_n(t))\left(\frac{d}{dt}u_n(t)\right)^2 \\ -\Omega^2\,r_m\,b\cos(\Omega t+\theta_{n-2})\sin(u_n(t))-\Omega^2\,r_m\,b\sin(\Omega t+\theta_{n-2})\cos(u_n(t)) \end{bmatrix}=0 \quad (5)$$

$$\left(\frac{d^2}{dt^2}u_n(t)\right)+\omega_n^2\,u_n(t)+r_b\,a\,\Omega^2\sin(u_n(t))-r_b\sin(\Omega t+\theta_{n-2})\cos(u_n(t))\left(\frac{d^2}{dt^2}u_1(t)\right)$$
$$-r_b\cos(\Omega t+\theta_{n-2})\sin(u_n(t))\left(\frac{d^2}{dt^2}u_1(t)\right)+r_b\,cos(\Omega t+\theta_{n-2})\cos(u_n(t))\left(\frac{d^2}{dt^2}u_2(t)\right) \quad (6)$$
$$-r_b\sin(\Omega t+\theta_{n-2})\sin(u_n(t))\left(\frac{d^2}{dt^2}u_2(t)\right)=0\,;\quad n=3...6$$

where $r_m=\dfrac{m_b}{m_f+Nb\,m_b}$, $r_b=1/b$, $\omega_1^2=\dfrac{K_{f\_X}}{m_f+Nb\,m_b}$, $\omega_2^2=\dfrac{K_{f\_Y}}{m_f+Nb\,m_b}$, $\omega_{3..6}^2=\dfrac{K_{b\_1..4}}{b^2\,m_b+Iz_b}$

The terms ω_1 and ω_2 are the resonance frequency of the fuselage in the *x* and *y* directions, respectively. Moreover, $\omega_{3..6}$ are the resonance frequencies of blades 1 to 4. The terms r_m and r_b are smaller than one.

3. FLOQUET'S METHOD

In this section a simplified mathematical model is expanded. A Taylor's series of first order is developed for the terms $\sin(u_n)$ and $\cos(u_n)$ in the equations (4-6) and, furthermore, the nonlinear terms are neglected. Consequently, a new dynamical system is reached, and is represented as below.

$$\mathbf{M}\,\ddot{\mathbf{u}}+\mathbf{G}\,\dot{\mathbf{u}}+\mathbf{K}\,\mathbf{u}=\mathbf{F_{ext}} \quad (7)$$

where $\mathbf{M}$ is the inertia matrix, $\mathbf{G}$ is the damping matrix, $\mathbf{K}$ is the stiffness matrix, and $\mathbf{F_{ext}}$ is the external vector force.

Due to the fact that parametric terms exist, $\mathbf{M}$ becomes a symmetric and non-diagonal matrix, $\mathbf{G}$ and $\mathbf{K}$ are non-symmetric and non-diagonal matrices. Also, because of the rotor head's symmetry, $\mathbf{F_{ext}}$ is equal to zero.

Then, Floquet's theory is used to solve differential equations with periodic coefficients. Considering **S**(t), the state-space matrix with period *T* of Eq. (7), and its state-space representation as

$$\dot{\mathbf{v}}(t)=\mathbf{S}(t)\,\mathbf{v}(t),\quad t>t_0$$
$$\mathbf{v}(t_0)=\mathbf{v}_0,\quad \mathbf{v}(t)=\left[\mathbf{u}(t)\quad \dot{\mathbf{u}}(t)\right]^T \quad (8)$$

By Floquet's Theory, a transition matrix $\mathbf{\Phi}$, which relates $\mathbf{v}(t)$ and $\mathbf{v}(t_0)$, is defined as

$$\mathbf{\Phi}(t,t_0)=\mathbf{P}(t,t_0)\,e^{(t-t_0)\,\mathbf{Q}} \quad (9)$$

The monodromy matrix **R** and the constant matrix **Q** are defined, then:

$$\mathbf{R}=\mathbf{\Phi}(t_0+T,t_0)\quad\text{and}\quad \mathbf{Q}=\frac{1}{T}\log(\mathbf{R}) \quad (10)$$

The dynamical system Eq. (7) is stable if the eigenvalues (μ) of **Q** are negative or, similarly, if the norm of the eigenvalues of **R** is less than one.

4. MULTIPLE SCALES METHOD

The perturbation method used to obtain the solution for these nonlinear equations is the multiple scales method (Nayfeh, 2004). It consists of assuming that in any function dependent of time, the independent variable *t* is a function of multiple scales of the time at the first order. Then, the perturbation substitutions created by introducing a bookkeeping parameter ε are:

$$\mathbf{u}_n(t) = \mathbf{u}_{n_0}(T_0, T_1) + \varepsilon\, \mathbf{u}_{n_1}(T_0, T_1) \quad n = 1..6; \tag{11}$$

$$r_m = \varepsilon\,\alpha, \quad r_b = \varepsilon\,\beta, \quad \Omega = \Omega_R + \varepsilon\,\sigma \tag{12}$$

where, Ω_R is the nominal rotor speed, σ is the detuning frequency parameter of the rotation speed and the terms T_0 and T_1 correspondent to t and $\varepsilon\, t$, respectively.

The terms $\sin(u_n)$ and $\cos(u_n)$ are expanded by a Taylor's series of first order in **u** and, after that, the perturbation substitutions are done on the equations of motion. Consequently, several sets of equations are obtained by grouping them by power of ε.

4.1. Order ε^0 equations

The set of order ε^0 equations of the system is collected. They represent the steady-state response of the uncoupled rotor and fuselage system.

$$\mathrm{D}_0^2\, u_{n_0}(T_0, T_1) + \omega_n^2\, u_{n_0}(T_0, T_1) = 0, \quad n = 1..6 \tag{13}$$

where D_0 is the derivative with respect to T_0.

The solutions of these equations are trivial and are in the form of $\left(u_{n_0} = \frac{1}{2} A_n(T_1)\, e^{I\,\omega_n T_0} + [c.c],\; n = 1..6 \right)$, since the steady-state responses are zero. The term $A_n(T_1)$ is complex and defined as $A_n(T_1) = C_n(T_1)\, e^{-I\, B_n(T_1)}$, where C_n and B_n are the amplitude and phase angle of each response, respectively.

4.2. Order ε^1 equations

The following, Eq. (14-16), is the set equations of order ε^1.

$$\begin{aligned}
&\mathrm{D}_0^2\, u_{1_1}(T_0, T_1) + \omega_1^2\, u_{1_1}(T_0, T_1) = \\
&\sum_{n=3}^{6} \left\{ \begin{aligned}
&\left[\begin{aligned} &\frac{1}{2} I^{(n-3)}\, \alpha\, b\, \mathrm{D}_0^2\, u_{n_0}(T_0, T_1)\, e^{I(\Omega_R T_0 + \sigma T_1)} + I^{(n-2)}\, \alpha\, b\, \Omega_R\, \mathrm{D}_0\, u_{n_0}(T_0, T_1)\, e^{I(\Omega_R T_0 + \sigma T_1)} \\ &+ \frac{1}{2} I^{(n-2)}\, \alpha\, b \left(\mathrm{D}_0\, u_{n_0}(T_0, T_1) \right)^2 e^{I(\Omega_R T_0 + \sigma T_1)} + \frac{1}{2} I^{(n-2)}\, \alpha\, b\, \Omega_R^2\, e^{I(\Omega_R T_0 + \sigma T_1)} \end{aligned} \right] u_{n_0}(T_0, T_1) \\
&+ \left[\begin{aligned} &-\frac{1}{2} I^{(n-2)}\, \alpha\, b\, \mathrm{D}_0^2\, u_{n_0}(T_0, T_1)\, e^{I(\Omega_R T_0 + \sigma T_1)} + I^{(n-3)}\, \alpha\, b\, \Omega_R\, \mathrm{D}_0\, u_{n_0}(T_0, T_1)\, e^{I(\Omega_R T_0 + \sigma T_1)} \\ &+ \frac{1}{2} I^{(n-3)}\, \alpha\, b \left(\mathrm{D}_0\, u_{n_0}(T_0, T_1) \right)^2 e^{I(\Omega_R T_0 + \sigma T_1)} \end{aligned} \right] + [c.c]
\end{aligned} \right\}
\end{aligned} \tag{14}$$

$$D_0^2\, u_{2\,1}(T_0,T_1)+\omega_2^2 u_{2\,1}(T_0,T_1)=$$

$$\sum_{n=3}^{6}\left\{\begin{array}{l}\left[\begin{array}{l}-\frac{1}{2}I^{(n-2)}\,\alpha b\, D_0^2\, u_{n\,0}(T_0,T_1)e^{I(\Omega_R T_0+\sigma T_1)}+I^{(n-3)}\,\alpha b\,\Omega_R\, D_0\, u_{n\,0}(T_0,T_1)e^{I(\Omega_R T_0+\sigma T_1)}\\ +\frac{1}{2}I^{(n-3)}\,\alpha b\left(D_0\, u_{n\,0}(T_0,T_1)\right)^2 e^{I(\Omega_R T_0+\sigma T_1)}+\frac{1}{2}I^{(n-3)}\,\alpha b\,\Omega_R^2\, e^{I(\Omega_R T_0+\sigma T_1)}\end{array}\right]u_{n\,0}(T_0,T_1)\\ +\left[\begin{array}{l}-\frac{1}{2}I^{(n-3)}\,\alpha b\, D_0^2\, u_{n\,0}(T_0,T_1)e^{I(\Omega_R T_0+\sigma T_1)}-I^{(n-2)}\,\alpha b\,\Omega_R\, D_0\, u_{n\,0}(T_0,T_1)e^{I(\Omega_R T_0+\sigma T_1)}\\ -\frac{1}{2}I^{(n-2)}\,\alpha b\left(D_0\, u_{n\,0}(T_0,T_1)\right)^2 e^{I(\Omega_R T_0+\sigma T_1)}\end{array}\right]+[c.c]\end{array}\right\} \quad (15)$$

$$D_0^2\, u_{n\,1}(T_0,T_1)+\omega_n^2\, u_{n\,1}(T_0,T_1)=$$

$$\left[\frac{1}{2}I^{(n-3)}\,\beta D_0^2\, u_{1\,0}(T_0,T_1)e^{I(\Omega_R T_0+\sigma T_1)}-\frac{1}{2}I^{(n-2)}\,\beta D_0^2\, u_{2\,0}(T_0,T_1)e^{I(\Omega_R T_0+\sigma T_1)}\right]u_{n\,0}(T_0,T_1)+ \quad (16)$$

$$-\frac{1}{2}I^{(n-2)}\beta D_0^2\, u_{1\,0}(T_0,T_1)e^{I(\Omega_R T_0+\sigma T_1)}-\frac{1}{2}I^{(n-3)}\,\beta D_0^2\, u_{2\,0}(T_0,T_1)e^{I(\Omega_R T_0+\sigma T_1)}+[c.c] \qquad n=3..6$$

where [c.c] corresponds to the complex conjugate of the previous terms.

As observed, the right-hand side of the above equations is all dependent on the steady-state responses $u_{n\,0}$.

4.3. Secular terms – possible instable regions

The developing of Eq. (14-16), after Eq. (13) have been substituted into them, lead to combinations of ω_n and Ω_R multiplied by T_0 as exponent to each equation of motion. Therefore, depending on the applied specific rotor speed Ω_R , secular terms may exist. This fact implies that the response(s) $u_{n\,1}$ grows without limit as t increases and, consequently, it does not provide a small correction to $u_{n\,0}$.

Based on that, a set of possible rotor speed values of Ω_R for each equation is listed and it indicates instability zones of the system. These zones are well defined through the analysis of the amplitude responses calculated around a critical value for Ω_R by shifting the detuning frequency parameter.

Body's Equation – Eq. (14): $\left[0 \quad \omega_1 \quad |\omega_1 \pm \omega_n| \quad |\omega_1 \pm 2\,\omega_n| \quad |\omega_1 \pm 3\,\omega_n|\right] \quad n=3..6$ (17)

Body's Equation – Eq. (15): $\left[0 \quad \omega_2 \quad |\omega_2 \pm \omega_n| \quad |\omega_2 \pm 2\,\omega_n| \quad |\omega_2 \pm 3\,\omega_n|\right] \quad n=3..6$ (18)

Blade's Equations – Eq. (16): $\left[\omega_{1,2} \quad |\omega_{1,2} - \omega_n| \quad |\omega_{1,2} - 2\,\omega_n|\right] \quad n=3..6$ (19)

5. RESULTS

The goal of this section is to predict and collect the speed rotor value Ω_R for which the system becomes instable from both mathematical models developed previously. Later, the results are compared.

The numerical values used for the system's inputs are defined in Tab. 1.

Table 1. Numerical values of the fuselage and rotor head inputs

Fuselage	Rotor		
m_f = 2902.9 [kg]	m_b = 31.9 [kg]	a = 0.2 [m]	b = 2.5 [m]
$K_{f\text{-}X}$ = $K_{f\text{-}Y}$ = 1.077e3 [kN/m]	$K_{b\text{-}1..4}$ = 40.716 [kNm/rad]	I_{zb} = 259 [kg m^2]	

Applying the numerical values, the resonance frequency, in Hz, of the fuselage ω_1 and ω_2 are equal to 3.00 and, for the blades $\omega_3, \omega_4, \omega_5$ and ω_6 are equal to 1.50. By varying the rotor speed from 0 to 7 Hz, Fig. 2 illustrates the instability zone for 4.358< Ω <5.187, in Hz, by using Floquet's Method. It is defined when the real part of the characteristic multipliers are positive and nonzero.

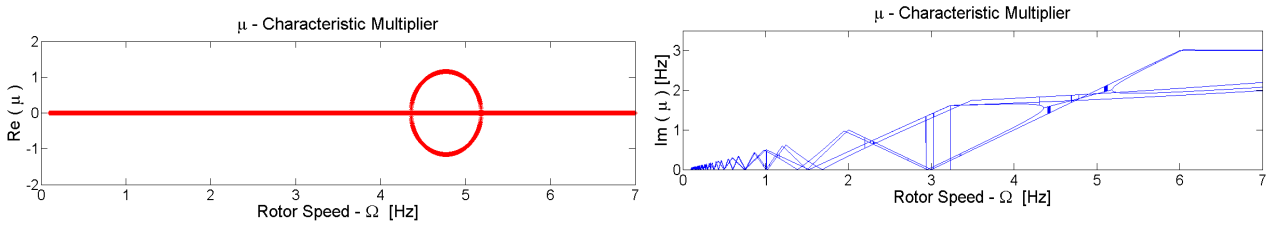

Figure 2. Campbell Diagram by Floquet Method.

However, by using Multiple Scales Method, the rotor speed values in Hz, at which unstable oscillations for the fuselage and the blades may occurs, are ordered as follow:

$$\Omega_R = [1.5 \quad 3.0 \quad 4.5 \quad 6.0 \quad 7.5] \tag{20}$$

6. CONCLUSION

As for the comprehension and analysis, this paper envisioned to verify the influence of the nonlinear terms in the equations of motion on the prediction of the rotor speed which the ground resonance phenomenon may occur. Two different models were developed and compared: one keeps the linear, parametric and periodic terms and another considers all terms, including the nonlinear ones.

The numerical results obtained in the first model, by applying the Floquet's Theory, show a well defined instability zone for the rotor speed between 4.358 and 5.187 Hz. Time response analysis for Ω =4.77 Hz evidences the divergent behaviour of the fuselage displacement.

However, the analysis of the secular terms in the nonlinear model, by using multiple scales method, verifies many others possibilities of instability zones. They are defined as a combination of the resonance frequency of the fuselage and the blades', by considering the linear system of motion as uncoupled. It evidences the importance of considering the nonlinear terms into the model in order to predict the instability zones.

The perspectives for this work consist in studying the amplitude responses in function of the detuning frequency parameter. It is envisioned too the analysis of the sensibility of each unstable region and the amplitude response in terms of internal detuning frequency parameters.

A passive control and an experimental validation of the results, through an experimental set up, are envisioned.

7. REFERENCES

Byers,L., Gandhi,F., Rotor blade with radial orber', American Helicopter Society 62nd Annual Forum, Phoenix, May, 2006.

Coleman, R. P., Feingold, A. M., 'Theory of self-excited mechanical oscillations of helicopter rotors with hinged blades', NACA Rep. 1351, 1958.

Donham, R.E., Cardinale, S.Y., Sachs, I.B., Ground and air resonance characteristics of a soft inplane rigid rotor system, J. Amer. Helicopter Soc. 14 (4), 1969.

Dawson, S.P., An experimental investigation of the stability of a bearingless model rotor in hover, J. Amer. Helicopter Soc. 28 (4), 1983.

Hodges, D.H., An aeromechanical stability analysis for bearingless rotor helicopters, J. Amer. Helicopter Soc. 24 (1), 1979.

Kunz, D., Nonlinear Analysis of helicopter ground resonance, Nonlinear Analysis: Real World Applications 3 page: 383 – 395, 2002.

Lytwyn, R.T. , Miao, W., Woitch, W., Airborne and ground resonance of hingeless rotors, J. Amer.Helicopter Soc. 16 (2), 1969.

Nayfeh, A. H. and Mook, D. T., 'Nonlinear Oscillations', John Wiley, 2nd ed, 2004.

Skjoldan, P.F., Hansen, M.H., 'On the similarity of the Coleman and Lyapunov-Floquet transformations for modal analysis of bladed rotor structures', Journal of Sound and Vibration 327(424 - 439), 2009.

8. RESPONSIBILITY NOTICE

The authors are the only responsible for the printed material included in this paper.